

## Sequence of potentials lying between the U(5) and X(5) symmetries

Dennis Bonatsos,<sup>1,\*</sup> D. Lenis,<sup>1,†</sup> N. Minkov,<sup>2,‡</sup> P. P. Raychev,<sup>2,§</sup> and P. A. Terziev<sup>2,||</sup>

<sup>1</sup>*Institute of Nuclear Physics, N.C.S.R. "Demokritos" GR-15310 Aghia Paraskevi, Attiki, Greece*

<sup>2</sup>*Institute for Nuclear Research and Nuclear Energy, Bulgarian Academy of Sciences, 72 Tzarigrad Road, BG-1784 Sofia, Bulgaria*

(Received 14 October 2003; published 20 January 2004)

Starting from the original collective Hamiltonian of Bohr and separating the  $\beta$  and  $\gamma$  variables as in the X(5) model of Iachello, an exactly soluble model corresponding to a harmonic oscillator potential in the  $\beta$  variable [to be called X(5)- $\beta^2$ ] is constructed. Furthermore, it is proved that the potentials of the form  $\beta^{2n}$  (with  $n$  being an integer) provide a "bridge" between this new X(5)- $\beta^2$  model (occurring for  $n=1$ ) and the X(5) model (corresponding to an infinite well potential in the  $\beta$  variable, materialized for  $n \rightarrow \infty$ ). Parameter-free (up to overall scale factors) predictions for spectra and  $B(E2)$  transition rates are given for the potentials  $\beta^2$ ,  $\beta^4$ ,  $\beta^6$ ,  $\beta^8$ , corresponding to  $R_4=E(4)/E(2)$  ratios of 2.646, 2.769, 2.824, and 2.852, respectively, compared to the  $R_4$  ratios of 2.000 for U(5) and 2.904 for X(5). Hints about nuclei showing this behavior, as well as about potentials "bridging" the X(5) symmetry with SU(3) are briefly discussed.

DOI: 10.1103/PhysRevC.69.014302

PACS number(s): 21.60.Ev, 21.60.Fw, 21.10.Re

### I. INTRODUCTION

Models providing parameter-independent predictions for nuclear spectra and electromagnetic transition rates serve as useful benchmarks in nuclear theory. The recently introduced E(5) [1] and X(5) [2] models belong to this category, since their predictions for nuclear spectra (normalized to the excitation energy of the first excited state) and  $B(E2)$  transition rates [normalized to the  $B(E2)$  transition rate connecting the first excited state to the ground state] do not contain any free parameters. The E(5) model appears to be related to a phase transition from U(5) (vibrational) to O(6) ( $\gamma$ -unstable) nuclei [1], while X(5) is related to a phase transition from U(5) (vibrational) to SU(3) (prolate deformed) nuclei [2]. Both models originate (under certain simplifying assumptions) from the Bohr collective Hamiltonian [3], which is known to possess the U(5) symmetry of the five-dimensional (5D) harmonic oscillator [4].

In the present paper we study a sequence of potentials lying between the U(5) symmetry of the Bohr Hamiltonian and the X(5) model. The potentials, which are of the form  $u_{2n}(\beta) = \beta^{2n}/2$ , with  $n$  being an integer, are depicted in Fig. 1. For  $n=1$  an exactly soluble model with  $R_4=E(4)/E(2)$  ratio equal to 2.646 is obtained, while X(5) (which corresponds to an infinite well potential) occurs for  $n \rightarrow \infty$  [in practice,  $n=4$  is already quite close to X(5)]. Parameter-independent predictions for the spectra and  $B(E2)$  values (up to the overall scales mentioned above) are obtained for the potentials  $\beta^2$ ,  $\beta^4$ ,  $\beta^6$ ,  $\beta^8$ . In addition to providing a number of models giving predictions directly comparable to experiment, the present sequence of potentials shows the way for approach-

ing the X(5) symmetry from the direction of U(5) and gives a hint on how to approach the X(5) symmetry starting from SU(3).

In Sec. II of the present paper the exactly soluble model obtained with the  $\beta^2$  potential, to be called X(5)- $\beta^2$ , is introduced and compared to X(5), while in Sec. III a sequence of potentials lying between the X(5)- $\beta^2$  and X(5) models is considered. Numerical results for spectra and  $B(E2)$  transition rates are given for all these potentials, which lie between the U(5) symmetry of the Bohr Hamiltonian [3,4] and the X(5) model. A brief comparison to experimental data is given in Sec. IV, while in Sec. V perspectives for further theoretical work are discussed and the conclusions are summarized.

### II. X(5)- $\beta^2$ : A NEW EXACTLY SOLUBLE MODEL

#### A. The $\beta$ part of the spectrum

The original Bohr Hamiltonian [3] is

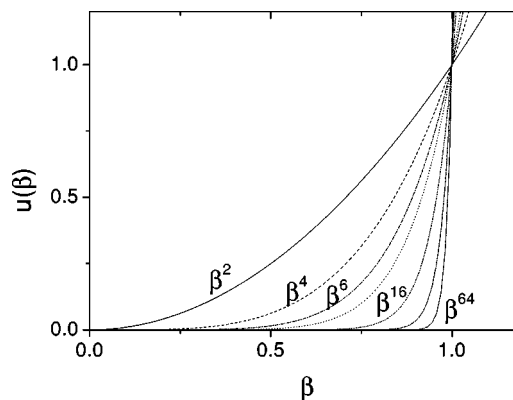


FIG. 1. The potentials  $\beta^{2n}$  with  $n=1$  (harmonic oscillator, solid line),  $n=2$  (dashed line),  $n=3$  (dash-dotted line),  $n=4$  (dotted line),  $n=8$  (dash-dot-dot),  $n=16$  (short dash-dot),  $n=32$  (short dot), gradually approaching (with increasing  $n$ ) the infinite well potential.

\*Email address: bonat@inp.demokritos.gr

†Email address: lenis@inp.demokritos.gr

‡Email address: nminkov@inrne.bas.bg

§Email address: raychev@phys.uni-sofia.bg,

raychev@inrne.bas.bg

||Email address: terziev@inrne.bas.bg

TABLE I. Spectra of the X(5)- $\beta^4$ , X(5)- $\beta^6$ , and X(5)- $\beta^8$  models, compared to the predictions of the X(5) [Eq. (6)] and X(5)- $\beta^2$  [Eq. (11)] models, for some  $s=1$  bands. See Secs. II C and III B for details. For the ( $n_\gamma=1$ ,  $K=2$ ) band the conventions of Ref. [8] have been used, as mentioned in Sec. II B.

Band	$L$	X(5)- $\beta^2$	X(5)- $\beta^4$	X(5)- $\beta^6$	X(5)- $\beta^8$	X(5)
$s=1, n_\gamma=0, K=0$						
	0	0.000	0.000	0.000	0.000	0.000
	2	1.000	1.000	1.000	1.000	1.000
	4	2.646	2.769	2.824	2.852	2.904
	6	4.507	4.929	5.125	5.230	5.430
	8	6.453	7.343	7.777	8.015	8.483
	10	8.438	9.954	10.721	11.151	12.027
	12	10.445	12.729	13.922	14.605	16.041
	14	12.465	15.647	17.359	18.355	20.514
	16	14.494	18.694	21.013	22.383	25.437
	18	16.529	21.858	24.871	26.677	30.804
	20	18.568	25.132	28.923	31.225	36.611
	22	20.610	28.506	33.159	36.017	42.853
	24	22.654	31.976	37.571	41.046	49.528
	26	24.700	35.536	42.151	46.302	56.633
	28	26.748	39.182	46.895	51.781	64.166
	30	28.796	42.909	51.795	57.475	72.124
$s=1, n_\gamma=1, K=2$						
	2	0.000	0.000	0.000	0.000	0.000
	3	0.907	0.925	0.932	0.936	0.943
	4	1.863	1.948	1.986	2.005	2.040
	5	2.842	3.046	3.138	3.186	3.274
	6	3.836	4.206	4.377	4.468	4.639
	7	4.839	5.420	5.694	5.842	6.127
	8	5.848	6.681	7.084	7.305	7.737
	9	6.860	7.986	8.543	8.850	9.465
	10	7.876	9.333	10.066	10.476	11.310

$$H = -\frac{\hbar^2}{2B} \left[ \frac{1}{\beta^4} \frac{\partial}{\partial \beta} \beta^4 \frac{\partial}{\partial \beta} + \frac{1}{\beta^2 \sin 3\gamma} \frac{\partial}{\partial \gamma} \sin 3\gamma \frac{\partial}{\partial \gamma} - \frac{1}{4\beta^2} \sum_{k=1,2,3} \frac{Q_k^2}{\sin^2\left(\gamma - \frac{2}{3}\pi k\right)} \right] + V(\beta, \gamma), \quad (1)$$

$$\sum_{k=1,2,3} \frac{Q_k^2}{\sin^2\left(\gamma - \frac{2\pi}{3}k\right)} \approx \frac{4}{3}(Q_1^2 + Q_2^2 + Q_3^2) + Q_3^2 \times \left( \frac{1}{\sin^2 \gamma} - \frac{4}{3} \right). \quad (2)$$

where  $\beta$  and  $\gamma$  are the usual collective coordinates, while  $Q_k$  ( $k=1, 2, 3$ ) are the components of angular momentum and  $B$  is the mass parameter.

One seeks solutions of the relevant Schrödinger equation having the form  $\Psi(\beta, \gamma, \theta_i) = \phi_K^L(\beta, \gamma) \mathcal{D}_{M,K}^L(\theta_i)$ , where  $\theta_i$  ( $i=1, 2, 3$ ) are the Euler angles,  $\mathcal{D}(\theta_i)$  denote Wigner functions of them,  $L$  are the eigenvalues of angular momentum, while  $M$  and  $K$  are the eigenvalues of the projections of angular momentum on the laboratory-fixed  $z$  axis and the body-fixed  $z'$  axis, respectively.

As pointed out in Ref. [2], in the case in which the potential has a minimum around  $\gamma=0$  one can write the last term of Eq. (1) in the form

Using this result in the Schrödinger equation corresponding to the Hamiltonian of Eq. (1), introducing reduced energies  $\epsilon = 2BE/\hbar^2$  and reduced potentials  $u = 2BV/\hbar^2$ , and assuming that the reduced potential can be separated into two terms, one depending on  $\beta$  and the other depending on  $\gamma$ , i.e.,  $u(\beta, \gamma) = u(\beta) + u(\gamma)$ , the Schrödinger equation can be separated into two equations [2]:

$$\left[ -\frac{1}{\beta^4} \frac{\partial}{\partial \beta} \beta^4 \frac{\partial}{\partial \beta} + \frac{1}{4\beta^2} L(L+1) + u(\beta) \right] \xi_L(\beta) = \epsilon_\beta \xi_L(\beta), \quad (3)$$

$$\left[ -\frac{1}{\langle \beta^2 \rangle \sin 3\gamma} \frac{\partial}{\partial \gamma} \sin 3\gamma \frac{\partial}{\partial \gamma} + \frac{1}{4\langle \beta^2 \rangle} K^2 \left( \frac{1}{\sin^2 \gamma} - \frac{4}{3} \right) + u(\gamma) \right] \eta_K(\gamma) = \epsilon(\gamma) \eta_K(\gamma), \quad (4)$$

where  $\langle \beta^2 \rangle$  is the average of  $\beta^2$  over  $\xi(\beta)$  and  $\epsilon = \epsilon_\beta + \epsilon_\gamma$ .

In Ref. [2] Eq. (3) is solved exactly for the case in which  $u(\beta)$  is an infinite well potential

$$u(\beta) = \begin{cases} 0 & \text{if } \beta \leq \beta_W \\ \infty & \text{for } \beta > \beta_W. \end{cases} \quad (5)$$

The relevant exactly soluble model is labeled as X(5) (which is not meant as a group label, although there is relation to projective representations of E(5), the Euclidean group in five dimensions [2]). In particular, Eq. (3) in the case of  $u(\beta)$  being an infinite well potential is transformed into a Bessel equation, the relevant eigenvalues being

$$\epsilon_{\beta,s,L} = (k_{s,L})^2, \quad k_{s,L} = \frac{x_{s,L}}{\beta_W}, \quad (6)$$

where  $x_{s,L}$  is the  $s$ th zero of the Bessel function  $J_\nu(k_{s,L}\beta)$ , with

$$\nu = \left( \frac{L(L+1)}{3} + \frac{9}{4} \right)^{1/2}, \quad (7)$$

while the relevant eigenfunctions are

$$\xi_{s,L}(\beta) = c_{s,L} \beta^{-3/2} J_\nu(k_{s,L}\beta), \quad (8)$$

where  $c_{s,L}$  are normalization constants.

Equation (3) is exactly soluble also in the case in which  $u(\beta) = \beta^2/2$ . In this case, to which we are going to refer as the X(5)- $\beta^2$  model, the eigenfunctions are [5]

$$F_n^L(\beta) = \left[ \frac{2n!}{\Gamma(n+a+\frac{5}{2})} \right]^{1/2} \beta^a L_n^{a+3/2}(\beta^2) e^{-\beta^2/2}, \quad (9)$$

where  $\Gamma(n)$  stands for the  $\Gamma$  function,  $L_n^a(z)$  denotes the Laguerre polynomials [6], and

$$a = \frac{1}{2} \left( -3 + \sqrt{9 + \frac{4}{3}L(L+1)} \right), \quad (10)$$

while the energy eigenvalues are

$$E_{n,L} = 2n + a + \frac{5}{2} = 2n + 1 + \sqrt{\frac{9}{4} + \frac{L(L+1)}{3}}, \quad (11)$$

$$n = 0, 1, 2, \dots \quad (11)$$

In the above,  $n$  is the usual oscillator quantum number. One can see that a formal correspondence between the energy levels of the X(5) model and the present X(5)- $\beta^2$  model can be established through the relation

$$n = s - 1. \quad (12)$$

It should be emphasized that Eq. (12) expresses just a formal one-to-one correspondence between the states in the two spectra, while the origin of the two quantum numbers is dif-

ferent,  $s$  labeling the order of a zero of a Bessel function and  $n$  labeling the number of zeros of a Laguerre polynomial. In the present notation, the ground state band corresponds to  $s = 1$  ( $n = 0$ ). For the energy states the notation  $E_{s,L} = E_{n+1,L}$  of Ref. [2] will be kept.

### B. The $\gamma$ part of the spectrum

In the original version of the X(5) model [2] the potential  $u(\gamma)$  in Eq. (4) is considered as a harmonic oscillator potential. The energy eigenvalues turn out to be

$$E(s, L, n_\gamma, K, M) = E_0 + B(x_{s,L})^2 + An_\gamma + CK^2, \quad (13)$$

where  $n_\gamma$  and  $K$  come from solving Eq. (4) for  $u(\gamma)$  being a harmonic oscillator potential

$$n_\gamma = 0, K = 0; \quad n_\gamma = 1, K = \pm 2; \quad n_\gamma = 2, K = 0, \pm 4; \dots \quad (14)$$

For  $K=0$  one has  $L=0, 2, 4, \dots$ , while for  $K \neq 0$  one obtains  $L=K, K+1, K+2, \dots$

A variation of the X(5) model is considered in Ref. [7], in which  $u(\gamma)$  is considered not as a harmonic oscillator, but as an infinite well

$$u(\gamma) = \begin{cases} 0 & \text{if } \gamma \leq \gamma_W \\ \infty & \text{for } \gamma > \gamma_W. \end{cases} \quad (15)$$

In this case the energy eigenvalues are given by

$$E(s, L, s', K, M) = A(x_{s,L})^2 + B(x_{s',K})^2 - 0.89AK^2, \quad (16)$$

where  $x_{s',K}$  is the  $s'$ th zero of the Bessel function  $J_{\nu'}(k_{s',K}\gamma)$ , with

$$\nu' = \frac{K}{2}, \quad k_{s',K} = \frac{x_{s',K}}{\gamma_W}, \quad (k_{s',K})^2 = \epsilon_{\gamma,s',K}. \quad (17)$$

In the present X(5)- $\beta^2$  model, one can keep in Eq. (4) for  $u(\gamma)$  a harmonic oscillator potential, as in the X(5) model. As a consequence, the full spectrum is given by

$$E(n, L, n_\gamma, K, M) = E'_0 + B' \left( 2n + 1 + \sqrt{\frac{L(L+1)}{3} + \frac{9}{4}} \right) + A'n_\gamma + C'K^2, \quad (18)$$

which is an analog of Eq. (13). Equation (14) and the discussion following it remain unchanged.

Yet another variation of the X(5) model is considered in Ref. [8]. In this case, when performing the separation of variables in Eq. (1) by using Eq. (2), one keeps the  $4K^2/3$  term in Eq. (3) instead of Eq. (4). As a result, in Eq. (3) the term  $L(L+1) - K^2$  appears in the place of  $L(L+1)$ , and the same substitution occurs as a consequence in Eqs. (7), (10), (11), and (18). In addition, the term  $4K^2/3$  disappears from Eq. (4) and, as a consequence, the term containing  $K^2$  is eliminated in Eqs. (13), (16), and (18).

TABLE II. Same as Table I, but for some  $s > 1$  bands.

Band	$L$	$X(5)-\beta^2$	$X(5)-\beta^4$	$X(5)-\beta^6$	$X(5)-\beta^8$	$X(5)$
$s=2, n_\gamma=0, K=0$						
	0	3.562	4.352	4.816	5.091	5.649
	2	4.562	5.602	6.232	6.619	7.450
	4	6.208	7.733	8.684	9.288	10.689
	6	8.069	10.248	11.629	12.527	14.751
	8	10.014	12.990	14.896	16.154	19.441
	10	11.999	15.901	18.419	20.100	24.687
	12	14.007	18.951	22.168	24.331	30.454
	14	16.027	22.125	26.121	28.827	36.723
	16	18.056	25.409	30.267	33.573	43.481
	18	20.091	28.796	34.594	38.559	50.719
	20	22.129	32.278	39.094	43.777	58.429
$s=3, n_\gamma=0, K=0$						
	0	7.123	9.384	10.823	11.758	14.119
	2	8.123	10.817	12.562	13.710	16.716
	4	9.769	13.228	15.520	17.054	21.271
	6	11.630	16.032	19.004	21.025	26.832
	8	13.576	19.050	22.802	25.385	33.103
	10	15.561	22.221	26.838	30.051	39.979
	12	17.568	25.514	31.079	34.983	47.413
	14	19.589	28.916	35.504	40.161	55.377
	16	21.617	32.416	40.103	45.571	63.856
	18	23.652	36.007	44.866	51.202	72.838
	20	25.691	39.683	49.786	57.047	82.315
$s=4, n_\gamma=0, K=0$						
	0	10.685	14.956	17.831	19.781	25.414
	2	11.685	16.536	19.842	22.105	28.805
	4	13.331	19.177	23.235	26.044	34.669
	6	15.192	22.225	27.189	30.667	41.717
	8	17.137	25.483	31.458	35.689	49.551
	10	19.123	28.882	35.955	41.009	58.033
	12	21.130	32.394	40.643	46.584	67.100
	14	23.150	36.002	45.501	52.392	76.721
	16	25.179	39.699	50.519	58.419	86.876
	18	27.214	43.478	55.689	64.653	97.552
	20	29.253	47.334	61.003	71.089	108.739

**C. Numerical spectra**

Numerical results for the  $\beta$  parts of the energy spectra (which correspond to no excitations in the  $\gamma$  variable, i.e., to  $n_\gamma=0$ ) of the  $X(5)-\beta^2$  and  $X(5)$  models are shown in Tables I and II. All levels are normalized to the energy of the first excited state,  $E_{1,2}-E_{1,0}=1.0$ , where the notation  $E_{s,L}=E_{n+1,L}$  is used. The model predictions for these bands are parameter independent, up to an overall scale, as seen from Eqs. (6) and (11). This is not the case for bands with  $n_\gamma \neq 0$ , since in this case, as seen from Eqs. (13) and (18) the

extra parameters  $A, C$  and  $A', C'$  enter, respectively. Therefore, in the case of the ( $n_\gamma=1, K=2$ ) band, the energies are listed in Table I after subtracting from them the relevant  $L=2$  bandhead, using the same normalization as above. In the case of the ( $n_\gamma=1, K=2$ ) band, the conventions of Ref. [8], described at the end of the preceding subsection, have been used. The  $K=0$  bands are not affected by these conventions, anyway.

A comparison between the spectra of the  $X(5)-\beta^2$  and  $X(5)$  models, given in Tables I and II, leads to the following observations.

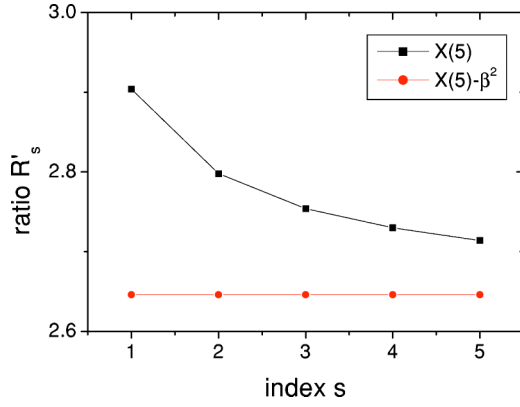


FIG. 2. (Color online) The energy ratio  $R'_s$ , defined in Eq. (21), for the X(5) and X(5)- $\beta^2$  models. See Sec. II C for further discussion.

(a) The members of the ground state band are characterized by the ratios

$$R_L = \frac{E_{1,L} - E_{1,0}}{E_{1,2} - E_{1,0}}. \quad (19)$$

The  $R_4$  ratio within the ground state band is 2.646 in the case of X(5)- $\beta^2$ , as compared to 2.904 in the case of X(5). Furthermore, all normalized energy levels within the ground state band of X(5)- $\beta^2$  are lower than the corresponding X(5) normalized energy levels. The same holds within the  $n_\gamma=1$  bands. Therefore X(5)- $\beta^2$  corresponds to nuclei “less rotational” than the ones corresponding to X(5).

(b) The location of the bandheads of the various  $s$  families is described by the ratios

$$\bar{R}_s = \frac{E_{s,0} - E_{1,0}}{E_{1,2} - E_{1,0}}. \quad (20)$$

The  $\bar{R}_2$  ratio, related to the position of the bandhead of the  $s=2$  band, is 3.562 in X(5)- $\beta^2$ , while it is 5.649 in X(5). In other words, the  $s=2$  bandhead in X(5)- $\beta^2$  lies much lower than in X(5). The same holds for all bandheads of  $s$  families, as seen in Table II.

(c) The  $s=2$  bandhead in X(5)- $\beta^2$  lies almost midway between the  $4_1^+$  state and the  $6_1^+$  state of the ground state band ( $E_{1,4}$  and  $E_{1,6}$ , respectively), while in X(5) the  $s=2$  bandhead is almost degenerate with the  $6_1^+$  state ( $E_{1,6}$ ) of the ground state band. Indeed, in the case of X(5)- $\beta^2$  one has from Eq. (19) that  $R_4=2.646$  and  $R_6=4.507$ , their midway being 3.577, as compared to 3.562, which is the position of the  $s=2$  bandhead.

A difference between the X(5)- $\beta^2$  and X(5) models can be seen by considering the ratios [2]

$$R'_s = \frac{E_{s,4} - E_{s,0}}{E_{s,2} - E_{s,0}}. \quad (21)$$

In the X(5) case one obtains the series

$$R'_{s=1,2,3,\dots} = 2.904, 2.798, 2.754, 2.730, 2.714, \dots \quad (22)$$

In addition, the following limit holds:

$$\lim_{s \rightarrow \infty} R'_s = 2.646. \quad (23)$$

In contrast, in the framework of the X(5)- $\beta^2$  model the  $R'_s$  ratios are independent of  $s=n+1$ ,

$$R'_s{}^{\text{osc}} = \frac{\sqrt{\frac{107}{3}} - 3}{\sqrt{17} - 3} \approx 2.646. \quad (24)$$

In the case of a simple 5D harmonic oscillator this ratio would have been equal to 2.

The various ratios are shown in Fig. 2. We remark that in the X(5) model the rotational collectivity of the bands decreases with increasing  $s$  (a fact already mentioned in Ref. [2]), while in the X(5)- $\beta^2$  model the rotational collectivity remains invariant with increasing  $n=s-1$ . Furthermore, the X(5)- $\beta^2$  constant value of the  $R'_s{}^{\text{osc}}$  ratio is the limiting value of the X(5)  $R'_s$  ratio for  $s \rightarrow \infty$ .

#### D. $B(E2)$ transition rates

In nuclear structure it is well known that electromagnetic transition rates are quantities sensitive to the details of the underlying microscopic structure, as well as to details of the theoretical models, much more than the corresponding spectra. It is therefore a must to calculate  $B(E2)$  ratios [normalized to  $B(E2:2_1^+ \rightarrow 0_1^+) = 100$ ] for the X(5) and X(5)- $\beta^2$  models.

The quadrupole operator has the form [9]

$$T_\mu^{(E2)} = t\beta \left[ \mathcal{D}_{\mu,0}^{(2)}(\theta_i) \cos \gamma + \frac{1}{\sqrt{2}} [\mathcal{D}_{\mu,2}^{(2)}(\theta_i) + \mathcal{D}_{\mu,-2}^{(2)}(\theta_i)] \sin \gamma \right], \quad (25)$$

where  $t$  is a scale factor, while the  $B(E2)$  transition rates are given by

$$B(E2; L_s \rightarrow L'_s) = \frac{|\langle L_s || T^{(E2)} || L'_s \rangle|^2}{2L_s + 1}. \quad (26)$$

The matrix elements of the quadrupole operator involve an integral over the Euler angles, which is the same as in Ref. [2] and is performed by using the properties of the Wigner  $\mathcal{D}$  functions, of which only  $\mathcal{D}_{\mu,0}^{(2)}$  participates, since  $\gamma \approx 0$  in Eq. (25) [as mentioned before Eq. (2)], as well as an integral over  $\beta$ . After performing the integrations over the angles one is left with

$$B(E2; L_s \rightarrow L'_s) = (L_s 2 L'_s | 000)^2 T_{s, L_s; s', L'}^2, \quad (27)$$

where the Clebsch-Gordan coefficient  $(L_s 2 L'_s | 000)$  appears, which determines the relevant selection rules. In the case of X(5) the integral over  $\beta$  is

TABLE III. Intradband  $B(E2)$  transition rates for the  $X(5)-\beta^4$ ,  $X(5)-\beta^6$ , and  $X(5)-\beta^8$  models, compared to the predictions of the  $X(5)$  and  $X(5)-\beta^2$  models. See Secs. II D and III C for details.

Band	$(L_s)_i$	$(L_s)_f$	$X(5)-\beta^2$	$X(5)-\beta^4$	$X(5)-\beta^6$	$X(5)-\beta^8$	$X(5)$
$(s=1) \rightarrow (s=1)$							
	2 <sub>1</sub>	0 <sub>1</sub>	100.00	100.00	100.00	100.00	100.00
	4 <sub>1</sub>	2 <sub>1</sub>	177.90	169.03	165.31	163.41	159.89
	6 <sub>1</sub>	4 <sub>1</sub>	255.18	226.15	214.62	208.83	198.22
	8 <sub>1</sub>	6 <sub>1</sub>	337.06	279.88	258.09	247.31	227.60
	10 <sub>1</sub>	8 <sub>1</sub>	421.32	330.45	297.02	280.71	250.85
	12 <sub>1</sub>	10 <sub>1</sub>	506.85	378.25	332.37	310.24	269.73
	14 <sub>1</sub>	12 <sub>1</sub>	593.11	423.67	364.85	336.77	285.42
	16 <sub>1</sub>	14 <sub>1</sub>	679.84	467.07	395.01	360.94	298.69
	18 <sub>1</sub>	16 <sub>1</sub>	766.88	508.74	423.25	383.18	310.11
	20 <sub>1</sub>	18 <sub>1</sub>	854.13	548.89	449.86	403.84	320.04
	22 <sub>1</sub>	20 <sub>1</sub>	941.54	587.72	475.10	423.16	328.79
	24 <sub>1</sub>	22 <sub>1</sub>	1029.06	625.37	499.14	441.35	336.57
	26 <sub>1</sub>	24 <sub>1</sub>	1116.68	661.98	522.13	458.56	343.54
	28 <sub>1</sub>	26 <sub>1</sub>	1204.36	697.64	544.19	474.91	349.84
	30 <sub>1</sub>	28 <sub>1</sub>	1292.10	732.44	565.43	490.49	355.55
$(s=2) \rightarrow (s=2)$							
	2 <sub>2</sub>	0 <sub>2</sub>	155.69	121.99	106.03	97.23	79.52
	4 <sub>2</sub>	2 <sub>2</sub>	240.30	187.73	162.89	149.05	120.02
	6 <sub>2</sub>	4 <sub>2</sub>	316.27	239.86	205.80	187.08	146.75
	8 <sub>2</sub>	6 <sub>2</sub>	397.68	290.57	245.80	221.73	169.31
	10 <sub>2</sub>	8 <sub>2</sub>	481.90	339.23	282.84	253.23	188.55
	12 <sub>2</sub>	10 <sub>2</sub>	567.55	385.73	317.15	281.93	205.12
	14 <sub>2</sub>	12 <sub>2</sub>	653.98	430.22	349.09	308.22	219.55
	16 <sub>2</sub>	14 <sub>2</sub>	740.88	472.91	379.00	332.49	232.24
	18 <sub>2</sub>	16 <sub>2</sub>	828.08	514.03	407.16	355.03	243.52
	20 <sub>2</sub>	18 <sub>2</sub>	915.48	553.74	433.81	376.11	253.63
$(s=3) \rightarrow (s=3)$							
	2 <sub>3</sub>	0 <sub>3</sub>	211.85	144.41	116.82	102.55	72.52
	4 <sub>3</sub>	2 <sub>3</sub>	302.74	208.42	169.03	148.48	104.36
	6 <sub>3</sub>	4 <sub>3</sub>	377.38	256.28	206.61	180.79	124.81
	8 <sub>3</sub>	6 <sub>3</sub>	458.35	304.07	242.92	211.42	142.94
	10 <sub>3</sub>	8 <sub>3</sub>	542.55	350.70	277.41	240.11	159.02
	12 <sub>3</sub>	10 <sub>3</sub>	628.33	395.71	309.93	266.81	173.30
	14 <sub>3</sub>	12 <sub>3</sub>	714.93	439.06	340.58	291.71	186.06
	16 <sub>3</sub>	14 <sub>3</sub>	802.00	480.86	369.55	314.99	197.54
	18 <sub>3</sub>	16 <sub>3</sub>	889.36	521.25	397.03	336.85	207.93
	20 <sub>3</sub>	18 <sub>3</sub>	976.92	560.37	423.18	357.46	217.41
$(s=4) \rightarrow (s=4)$							
	2 <sub>4</sub>	0 <sub>4</sub>	268.23	165.90	127.76	108.86	69.06
	4 <sub>4</sub>	2 <sub>4</sub>	365.19	229.20	177.27	151.33	95.96
	6 <sub>4</sub>	4 <sub>4</sub>	438.49	273.60	210.90	179.61	112.50
	8 <sub>4</sub>	6 <sub>4</sub>	519.04	318.87	244.18	207.11	127.62
	10 <sub>4</sub>	8 <sub>4</sub>	603.25	363.62	276.37	233.38	141.39
	12 <sub>4</sub>	10 <sub>4</sub>	689.16	407.17	307.10	258.20	153.88
	14 <sub>4</sub>	12 <sub>4</sub>	775.94	449.36	336.35	281.61	165.22

TABLE III. (Continued.)

Band	$(L_s)_i$	$(L_s)_f$	X(5)- $\beta^2$	X(5)- $\beta^4$	X(5)- $\beta^6$	X(5)- $\beta^8$	X(5)
	16 <sub>4</sub>	14 <sub>4</sub>	863.19	490.22	364.21	303.71	175.57
	18 <sub>4</sub>	16 <sub>4</sub>	950.72	529.83	390.81	324.64	185.07
	20 <sub>4</sub>	18 <sub>4</sub>	1038.42	568.29	416.27	344.52	193.82

$$I_{s,L;s',L'} = \int \beta \xi_{s,L}(\beta) \xi_{s',L'}(\beta) \beta^4 d\beta, \quad (28)$$

which, as seen from Eq. (8), involves Bessel functions, while in the case of X(5)- $\beta^2$  the integral has the form

$$I_{s,L;s',L'} = \int \beta F_n^L(\beta) F_{n'}^{L'} \beta^4 d\beta \quad (29)$$

with  $n=s-1$  and  $n'=s'-1$ , which involves Laguerre polynomials, as seen from Eq. (9).

The results for intraband transitions are reported in Table III, while interband transitions are listed in Table IV. All transitions are normalized to  $B(E2:2_1^+ \rightarrow 0_1^+) = 100$ . The following observations can be made.

(a) The ratio of the lowest  $B(E2)$ s within the ground state band

$$R_{4 \rightarrow 2} = \frac{B(E2:4_1^+ \rightarrow 2_1^+)}{B(E2:2_1^+ \rightarrow 0_1^+)} \quad (30)$$

is 1.7790 in X(5)- $\beta^2$ , while it is 1.5989 in X(5). In general, the normalized intraband  $B(E2)$ s in X(5)- $\beta^2$  are higher than the corresponding normalized  $B(E2)$ s in X(5). This is consistent with the fact that the various bands in X(5)- $\beta^2$  appear to be “less rotational” than the corresponding bands in X(5), as remarked above. It is well known from experimental data that in near-rotational nuclei the  $B(E2)$ s within the ground state band have high values which increase relatively slowly with increasing initial angular momentum, while in near-vibrational nuclei the  $B(E2)$ s within the ground state band have low values which increase rapidly with increasing initial angular momentum (in the absence of band crossings). This experimental picture is consistent with the intraband  $B(E2)$ s listed in Table III.

(b) As far as interband transitions are concerned, it is seen in Table IV that transitions which are strong in X(5) appear also to be strong in X(5)- $\beta^2$ , while transitions weak in X(5) are weak in X(5)- $\beta^2$  as well.

### III. A SEQUENCE OF POTENTIALS LYING BETWEEN U(5) AND X(5)

#### A. General

The two cases mentioned in the preceding section are the only ones in which Eq. (3) is exactly soluble, giving spectra characterized by  $R_4$  ratios 2.646 and 2.904 for X(5)- $\beta^2$  and X(5), respectively. However, the numerical solution of Eq. (3) for other potentials is a straightforward task. The poten-

tials to be used in Eq. (3) have to obey the restrictions imposed by the 24 transformations mentioned in Ref. [3] and listed explicitly in Ref. [10].

A particularly interesting sequence of potentials is given by

$$u_{2n}(\beta) = \frac{\beta^{2n}}{2}, \quad (31)$$

with  $n$  being an integer. For  $n=1$  the X(5)- $\beta^2$  case is obtained, while for  $n \rightarrow \infty$  the infinite well of X(5) is obtained [11], as shown in Fig. 1. Therefore this sequence of potentials interpolates between the X(5)- $\beta^2$  model and the X(5) model, in the region lying between U(5) and X(5).

#### B. Spectra

Numerical results for the spectra of the  $\beta^4$ ,  $\beta^6$ , and  $\beta^8$  potentials have been obtained through two different methods. In one approach, the representation of the position and momentum operators in matrix form [12] has been used, while in the other the direct integration method [13] has been applied. In the latter, the differential equation is solved for each value of  $L$  separately, the successive eigenvalues for each value of  $L$  labeled by  $s=1, 2, 3, \dots$  (or, equivalently, by  $n=0, 1, 2, \dots$ ). The two methods give results mutually consistent, the second one appearing of more general applicability. The results are shown in Tables I and II, where excitation energies relative to the ground state, normalized to the excitation energy of the first excited state, are exhibited.

In Tables I and II the model labels X(5)- $\beta^4$ , X(5)- $\beta^6$ , X(5)- $\beta^8$  have been used for the above-mentioned potentials, their meaning being that the X(5)- $\beta^{2n}$  model corresponds to the potential  $\beta^{2n}/2$  plugged in the differential equation (3) obtained in the framework of the X(5) model. In this notation X(5)- $\beta^{2n}$  with  $n \rightarrow \infty$  is simply the original X(5) model [2].

From Tables I and II it is clear that in all bands and for all values of the angular momentum  $L$ , the potentials  $\beta^4$ ,  $\beta^6$ ,  $\beta^8$  gradually lead from the X(5)- $\beta^2$  case to the X(5) results in a smooth way. The same conclusion is drawn from Fig. 3(a), where several levels of the ground state band of each model are shown versus the angular momentum  $L$ , as well as from Fig. 3(b), where the bandheads of several excited bands are shown for each model as a function of the index  $s$ .

#### C. $B(E2)$ transition rates

The calculation of the  $B(E2)$ s follows the steps described in Sec. II D. Equation (27) is still valid, the only difference being that in the integral over  $\beta$  the wave functions in the present cases are known only in numerical form and not in analytic form as in Eqs. (28) and (29).

TABLE IV. Same as Table III, but for interband transitions.

Band	$(L_s)_i$	$(L_s)_f$	$X(5)-\beta^2$	$X(5)-\beta^4$	$X(5)-\beta^6$	$X(5)-\beta^8$	$X(5)$
$(s=2) \rightarrow (s=1)$							
	0 <sub>2</sub>	2 <sub>1</sub>	121.92	93.21	81.03	74.66	62.41
	2 <sub>2</sub>	0 <sub>1</sub>	1.57	2.04	2.18	2.21	2.12
	2 <sub>2</sub>	2 <sub>1</sub>	13.40	11.34	10.28	9.66	8.22
	2 <sub>2</sub>	4 <sub>1</sub>	96.85	65.53	53.55	47.59	36.56
	4 <sub>2</sub>	2 <sub>1</sub>	0.06	0.48	0.72	0.84	0.94
	4 <sub>2</sub>	4 <sub>1</sub>	12.41	9.63	8.37	7.68	6.10
	4 <sub>2</sub>	6 <sub>1</sub>	96.68	59.53	46.23	39.78	27.87
	6 <sub>2</sub>	4 <sub>1</sub>	0.03	0.16	0.37	0.49	0.64
	6 <sub>2</sub>	6 <sub>1</sub>	12.32	8.84	7.41	6.64	4.92
	6 <sub>2</sub>	8 <sub>1</sub>	95.89	54.68	40.71	34.09	21.85
	8 <sub>2</sub>	6 <sub>1</sub>	0.12	0.08	0.27	0.39	0.56
	8 <sub>2</sub>	8 <sub>1</sub>	12.34	8.29	6.72	5.90	4.09
	8 <sub>2</sub>	10 <sub>1</sub>	95.03	50.85	36.56	29.91	17.64
	10 <sub>2</sub>	8 <sub>1</sub>	0.19	0.05	0.23	0.35	0.52
	10 <sub>2</sub>	10 <sub>1</sub>	12.37	7.86	6.19	5.35	3.49
	10 <sub>2</sub>	12 <sub>1</sub>	94.30	47.79	33.36	26.76	14.61
$(s=3) \rightarrow (s=2)$							
	0 <sub>3</sub>	2 <sub>2</sub>	241.37	166.55	136.53	120.61	86.33
	2 <sub>3</sub>	0 <sub>2</sub>	2.74	3.20	3.19	3.11	2.66
	2 <sub>3</sub>	2 <sub>2</sub>	25.45	19.61	16.82	15.19	11.25
	2 <sub>3</sub>	4 <sub>2</sub>	193.64	120.83	94.54	81.36	54.01
	4 <sub>3</sub>	2 <sub>2</sub>	0.11	0.70	0.97	1.08	1.12
	4 <sub>3</sub>	4 <sub>2</sub>	23.75	17.14	14.27	12.67	8.83
	4 <sub>3</sub>	6 <sub>2</sub>	193.35	111.85	84.29	70.99	43.76
	6 <sub>3</sub>	4 <sub>2</sub>	0.04	0.22	0.47	0.59	0.71
	6 <sub>3</sub>	6 <sub>2</sub>	23.73	16.09	13.01	11.37	7.46
	6 <sub>3</sub>	8 <sub>2</sub>	191.71	104.04	75.89	62.68	36.03
	8 <sub>3</sub>	6 <sub>2</sub>	0.20	0.11	0.33	0.46	0.60
	8 <sub>3</sub>	8 <sub>2</sub>	23.89	15.32	12.07	10.39	6.44
	8 <sub>3</sub>	10 <sub>2</sub>	189.99	97.61	69.18	56.16	30.26
	10 <sub>3</sub>	8 <sub>2</sub>	0.33	0.07	0.28	0.41	0.56
	10 <sub>3</sub>	10 <sub>2</sub>	24.05	14.69	11.31	9.61	5.65
	10 <sub>3</sub>	12 <sub>2</sub>	188.51	92.33	63.80	50.99	25.87
$(s=3) \rightarrow (s=1)$							
	0 <sub>3</sub>	2 <sub>1</sub>	0.8371	0.0300	0.0461	0.1835	0.5852
	2 <sub>3</sub>	0 <sub>1</sub>	0.1178	0.0311	0.0036	0.0002	0.0213
	2 <sub>3</sub>	2 <sub>1</sub>	0.4123	0.0770	0.0063	0.0012	0.0546
	2 <sub>3</sub>	4 <sub>1</sub>	0.0170	0.0716	0.2433	0.3876	0.6769
	4 <sub>3</sub>	2 <sub>1</sub>	0.0059	0.0005	0.0033	0.0139	0.0605
	4 <sub>3</sub>	4 <sub>1</sub>	0.3111	0.0471	0.0012	0.0051	0.0733
	4 <sub>3</sub>	6 <sub>1</sub>	0.0049	0.1241	0.2795	0.4046	0.6616
	6 <sub>3</sub>	4 <sub>1</sub>	0.0022	0.0020	0.0107	0.0240	0.0790
	6 <sub>3</sub>	6 <sub>1</sub>	0.2554	0.0323	0.0001	0.0085	0.0866
	6 <sub>3</sub>	8 <sub>1</sub>	0.0169	0.1235	0.2503	0.3548	0.5907
	8 <sub>3</sub>	6 <sub>1</sub>	0.0090	0.0043	0.0129	0.0255	0.0833
	8 <sub>3</sub>	8 <sub>1</sub>	0.2165	0.0236	0.0000	0.0104	0.0930



TABLE IV. (Continued.)

Band	$(L_s)_i$	$(L_s)_f$	$X(5)-\beta^2$	$X(5)-\beta^4$	$X(5)-\beta^6$	$X(5)-\beta^8$	$X(5)$
	8 <sub>3</sub>	10 <sub>1</sub>	0.0220	0.1102	0.2134	0.3011	0.5207
	10 <sub>3</sub>	8 <sub>1</sub>	0.0130	0.0051	0.0126	0.0240	0.0824
	10 <sub>3</sub>	10 <sub>1</sub>	0.1877	0.0181	0.0002	0.0112	0.0949
	10 <sub>3</sub>	12 <sub>1</sub>	0.0231	0.0960	0.1813	0.2555	0.4610
<hr/>							
$(s=4) \rightarrow (s=3)$							
	0 <sub>4</sub>	2 <sub>3</sub>	359.75	228.92	179.59	154.38	99.18
	2 <sub>4</sub>	0 <sub>3</sub>	3.77	4.05	3.86	3.66	2.85
	2 <sub>4</sub>	2 <sub>3</sub>	36.92	26.34	21.65	19.06	12.76
	2 <sub>4</sub>	4 <sub>3</sub>	290.41	169.37	127.74	107.41	64.60
	4 <sub>4</sub>	2 <sub>3</sub>	0.14	0.84	1.12	1.22	1.17
	4 <sub>4</sub>	4 <sub>3</sub>	34.54	23.40	18.80	16.32	10.39
	4 <sub>4</sub>	6 <sub>3</sub>	290.00	158.78	116.23	96.05	54.31
	6 <sub>4</sub>	4 <sub>3</sub>	0.06	0.26	0.52	0.64	0.73
	6 <sub>4</sub>	6 <sub>3</sub>	34.61	22.27	17.49	14.98	9.05
	6 <sub>4</sub>	8 <sub>3</sub>	287.51	149.11	106.29	86.50	46.15
	8 <sub>4</sub>	6 <sub>3</sub>	0.27	0.12	0.36	0.49	0.60
	8 <sub>4</sub>	8 <sub>3</sub>	34.93	21.45	16.48	13.95	8.02
	8 <sub>4</sub>	10 <sub>3</sub>	284.90	140.88	98.06	78.69	39.76
	10 <sub>4</sub>	8 <sub>3</sub>	0.45	0.08	0.31	0.43	0.56
	10 <sub>4</sub>	10 <sub>3</sub>	35.24	20.74	15.63	13.08	7.19
	10 <sub>4</sub>	12 <sub>3</sub>	282.67	133.99	91.26	72.30	34.73

The results of the calculations for intraband transitions are shown in Table III, while interband transitions are shown in Table IV. In addition, the normalized  $B(E2)$  transition rates within the ground state band of each model are shown in Fig.

3(c). In all cases a smooth evolution from  $X(5)-\beta^2$  to  $X(5)$  is seen. Furthermore, the results are in agreement with general qualitative expectations: the more rotational the nucleus, the less rapid the increase (with increasing initial angular mo-

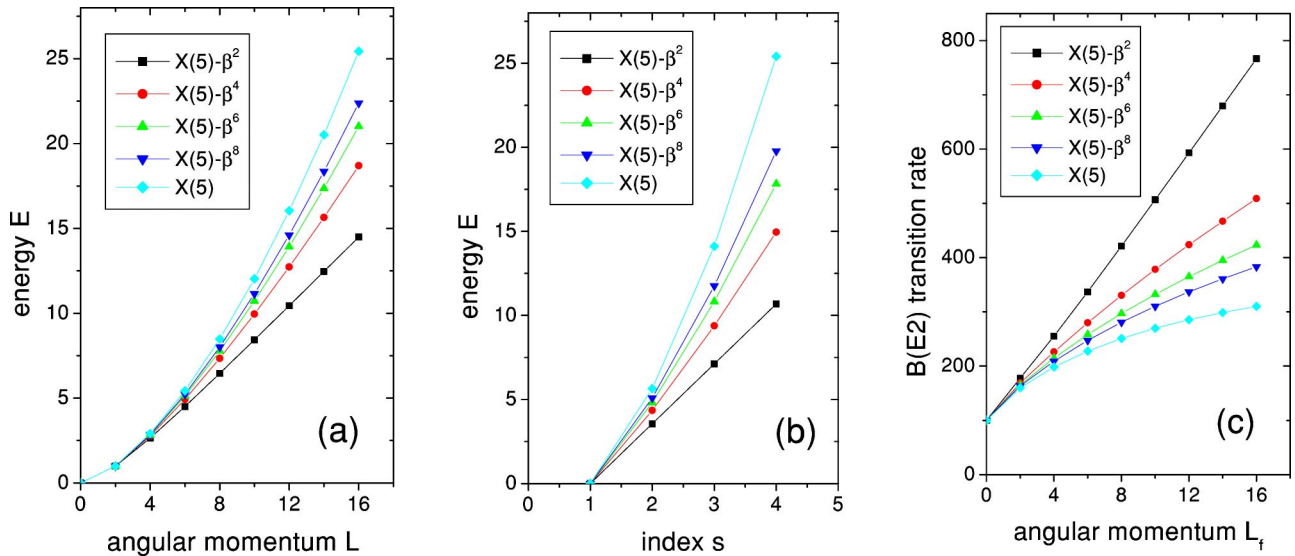


FIG. 3. (Color online) (a) Levels of the ground state bands of the models  $X(5)-\beta^{2n}$  with  $n=1-4$  and of the  $X(5)$  model, vs the angular momentum  $L$ . In each model all levels are normalized to the energy of the first excited state. See Sec. III B for further discussion. (b) Bandhead energies of excited bands of the same models and with the same normalization, vs the band index  $s$ . See Sec. III B for further discussion. (c)  $B(E2; L_f+2 \rightarrow L_f)$  transition rates within the ground state bands of the same models, vs the angular momentum of the final state,  $L_f$ . In each model all rates are normalized to the one between the lowest states,  $B(E2; 2 \rightarrow 0)$ . See Sec. III C for further discussion.

TABLE V. Experimental spectra of the ground state (g.s.) and  $\beta_1$  bands of  $^{148}\text{Nd}$  [17],  $^{160}\text{Yb}$  [19,20], and  $^{158}\text{Er}$  [18], compared to the predictions of the X(5)- $\beta^2$ , X(5)- $\beta^4$ , and X(5)- $\beta^6$  models, respectively.

Band	$L$	$^{148}\text{Nd}$	X(5)- $\beta^2$	$^{160}\text{Yb}$	X(5)- $\beta^4$	$^{158}\text{Er}$	X(5)- $\beta^6$
g.s.							
	2	1.000	1.000	1.000	1.000	1.000	1.000
	4	2.493	2.646	2.626	2.769	2.744	2.824
	6	4.242	4.507	4.718	4.929	5.050	5.125
	8	6.153	6.453	7.142	7.343	7.772	7.777
	10	8.194	8.438	9.761	9.954	10.786	10.721
	12	10.298	10.445	12.903	12.729	13.952	13.922
	14					17.561	17.359
$\beta_1$							
	0	3.039	3.562	4.463	4.352	4.197	4.816

mentum) of the  $B(E2)$  ratios within the ground state band should be. Indeed the most rapid increase is seen in the case of X(5)- $\beta^2$ , while the slowest increase is observed in the case of X(5).

**IV. COMPARISONS TO EXPERIMENTAL DATA**

From the above observations, we conclude that a few key features of the X(5)- $\beta^2$  model, which can serve as benchmarks in the search for nuclei exhibiting such behavior, are the following.

(a) The  $R_4$  ratio [defined in Eq. (19)] should be close to 2.646.

(b) The position of the  $s=2$  bandhead should be almost midway between the  $4_{1-}^+$  and  $6_1^+$  ( $E_{1,4}$  and  $E_{1,6}$ ) states of the ground state band, the  $R_2$  ratio [defined in Eq. (20) being 3.562].

(c) The ratio of the lowest  $B(E2)$ s within the ground state band,  $R_{4\rightarrow 2}$  [defined in Eq. (30)], should be around 1.7790.

Analogous remarks can be made in the cases of the X(5)- $\beta^4$ , X(5)- $\beta^6$ , and X(5)- $\beta^8$  models.

It is clear that the first place to look for nuclei exhibiting X(5)- $\beta^{2n}$  behavior is the region close to nuclei showing X(5) structure. The best examples of nuclei corresponding to the X(5) structure are so far the  $N=90$  isotones  $^{152}\text{Sm}$  [14],  $^{150}\text{Nd}$  [15],  $^{156}\text{Dy}$  [16]. A preliminary search in the rare earths with  $N < 90$  shows that  $^{148}\text{Nd}$  [17] can be a candidate for X(5)- $\beta^2$ ,  $^{158}\text{Er}$  [18] can be a candidate for X(5)- $\beta^6$ , while  $^{160}\text{Yb}$  [19,20] can be a candidate for X(5)- $\beta^4$ . Existing data for the ground state bands and the  $\beta_1$  bandheads of these nuclei are compared to the corresponding model predictions in Table V. However, much more detailed information on spectra and  $B(E2)$  transitions is needed before final conclusions can be reached.

**V. CONCLUSION**

An exactly soluble model, labeled as X(5)- $\beta^2$ , has been constructed starting from the original Bohr collective Hamil-

tonian, separating the  $\beta$  and  $\gamma$  variables as in the X(5) model of Iachello, and using a harmonic oscillator potential for the  $\beta$  variable. Furthermore it has been proved that the potentials  $\beta^{2n}$  (with  $n$  being an integer) provide a “bridge” between this new X(5)- $\beta^2$  model (occurring for  $n=1$ ) and the X(5) model of Iachello (which is obtained by putting in the Bohr Hamiltonian an infinite well potential in the  $\beta$  variable, materialized for  $n \rightarrow \infty$ ). Parameter-free (up to overall scale factors) predictions for spectra and  $B(E2)$  transition rates have been given for the potentials  $\beta^2$ ,  $\beta^4$ ,  $\beta^6$ ,  $\beta^8$ , called the X(5)- $\beta^2$ , X(5)- $\beta^4$ , X(5)- $\beta^6$ , and X(5)- $\beta^8$  models, respectively, lying between the U(5) symmetry of the original Bohr Hamiltonian and the X(5) model. Hints about nuclei showing this behavior have been given.

A sequence of potentials interpolating between the U(5) and E(5) symmetries should also be worked out. Furthermore, one should try to find a sequence of potentials interpolating between SU(3) and X(5), as well as between O(6) and E(5). In other words, one should try to approach E(5) and X(5) “from the other side.” From the classical limit of the O(6) and SU(3) symmetries of the Interacting Boson model [21] it is clear that for this purpose potentials with a minimum at  $\beta \neq 0$  should be considered, the Davidson-like potentials [22]

$$u_{2n}^D(\beta) = \beta^{2n} + \frac{\beta_0^{4n}}{\beta^{2n}} \tag{32}$$

being strong candidates. The Davidson potential, corresponding to  $n=1$ , is known to be exactly soluble [22,23]. Work in these directions is in progress.

**ACKNOWLEDGMENTS**

The authors are thankful to Rick Casten (Yale), Jean Libert (Orsay), and Werner Scheid (Giessen) for illuminating discussions. Support through a NATO Collaborative Linkage grant, Grant No. PST.CLG 978799, is gratefully acknowledged.

- [1] F. Iachello, Phys. Rev. Lett. **85**, 3580 (2000).
- [2] F. Iachello, Phys. Rev. Lett. **87**, 052502 (2001).
- [3] A. Bohr, Mat. Fys. Medd. K. Dan. Vidensk. Selsk. **26**, 14 (1952).
- [4] E. Chacón and M. Moshinsky, J. Math. Phys. **18**, 870 (1977).
- [5] M. Moshinsky, J. Math. Phys. **25**, 1555 (1984).
- [6] M. Abramowitz and I. A. Stegun, *Handbook of Mathematical Functions* (Dover, New York, 1965).
- [7] F. Iachello, in *Mapping the Triangle*, edited by Ani Aprahamian, Jolie A. Cizewski, Stuart Pittel, and N. Victor Zamfir, AIP Conf. Proc. No. 638 (AIP, Melville, NY, 2002), p. 1.
- [8] R. Bijker, R. F. Casten, N. V. Zamfir, and E. A. McCutchan, Phys. Rev. C (to be published).
- [9] L. Wilets and M. Jean, Phys. Rev. **102**, 788 (1956).
- [10] T. M. Corrigan, F. J. Margetan, and S. A. Williams, Phys. Rev. C **14**, 2279 (1976).
- [11] C. M. Bender, S. Boettcher, H. F. Jones, and V. M. Savage, J. Phys. A **32**, 6771 (1999).
- [12] H. J. Korsch and M. Glück, Eur. J. Phys. **23**, 413 (2002).
- [13] N. Minkov and W. Scheid, INRNE Sofia preprint, 2003.
- [14] R. F. Casten and N. V. Zamfir, Phys. Rev. Lett. **87**, 052503 (2001).
- [15] R. Krücken, B. Albanna, C. Bialik, R. F. Casten, J. R. Cooper, A. Dewald, N. V. Zamfir, C. J. Barton, C. W. Beausang, M. A. Caprio, A. A. Hecht, T. Klug, J. R. Novak, N. Pietralla, and P. von Brentano, Phys. Rev. Lett. **88**, 232501 (2002).
- [16] M. A. Caprio, N. V. Zamfir, R. F. Casten, C. J. Barton, C. W. Beausang, J. R. Cooper, A. A. Hecht, R. Krücken, H. Newman, J. R. Novak, N. Pietralla, A. Wolf, and K. E. Zyranski, Phys. Rev. C **66**, 054310 (2002).
- [17] M. R. Bhat, Nucl. Data Sheets **89**, 797 (2000).
- [18] R. G. Helmer, Nucl. Data Sheets **77**, 471 (1996).
- [19] C. W. Reich, Nucl. Data Sheets **78**, 547 (1996).
- [20] M. Sakai, At. Data Nucl. Data Tables **31**, 399 (1984).
- [21] F. Iachello and A. Arima, *The Interacting Boson Model* (Cambridge University Press, Cambridge, 1987).
- [22] P. M. Davidson, Proc. R. Soc. London, Ser. A **135**, 459 (1932).
- [23] D. J. Rowe and C. Bahri, J. Phys. A **31**, 4947 (1998).